Respiratory Research

RESEARCH

Open Access

Automated AI-based image analysis for quantification and prediction of interstitial lung disease in systemic sclerosis patients

Julien Guiot[1*], Monique Henket[1], Fanny Gester[1], Béatrice André[2], Benoit Ernst[1], Anne-Noelle Frix[1], Dirk Smeets[3], Simon Van Eyndhoven[3], Katerina Antoniou[4], Lennart Conemans[5], Janine Gote-Schniering[6,7], Hans Slabbynck[8], Michael Kreuter[9], Jacobo Sellares[10], Ioannis Tomos[11], Guang Yang[12,13], Clio Ribbens[2], Renaud Louis[1], Vincent Cottin[14], Sara Tomassetti[15], Vanessa Smith[16,17,18] and Simon L. F. Walsh[13]

Abstract

Background Systemic sclerosis (SSc) is a rare connective tissue disease associated with rapidly evolving interstitial lung disease (ILD), driving its mortality. Specific imaging-based biomarkers associated with the evolution of lung disease are needed to help predict and quantify ILD.

Methods We evaluated the potential of an automated ILD quantification system (icolung®) from chest CT scans, to help in quantification and prediction of ILD progression in SSc-ILD. We used a retrospective cohort of 75 SSc-ILD patients to evaluate the potential of the AI-based quantification tool and to correlate image-based quantification with pulmonary function tests and their evolution over time.

Results We evaluated a group of 75 patients suffering from SSc-ILD, either limited or diffuse, of whom 30 presented progressive pulmonary fibrosis (PPF). The patients presenting PPF exhibited more extensive lesions (in % of total lung volume (TLV)) based on image analysis than those without PPF: 3.93 (0.36–8.12)* vs. 0.59 (0.09–3.53) respectively, whereas pulmonary functional test showed a reduction in Force Vital Capacity (FVC)(pred%) in patients with PPF compared to the others : 77 ± 20% vs. 87 ± 19% ($p < 0.05$). Modifications of FVC and diffusing capacity of the lungs for carbon monoxide (DLCO) over time were correlated with longitudinal radiological ILD modifications (r=-0.40, $p < 0.01$; r=-0.40, $p < 0.01$ respectively).

Conclusion AI-based automatic quantification of lesions from chest-CT images in SSc-ILD is correlated with physiological parameters and can help in disease evaluation. Further clinical multicentric validation is necessary in order to confirm its potential in the prediction of patient's outcome and in treatment management.

Keywords Systemic sclerosis, Interstitial lung disease, Artificial intelligence, Computed tomography, Pulmonary function tests

*Correspondence:
Julien Guiot
J.Guiot@chuliege.be

Full list of author information is available at the end of the article

Background

Systemic sclerosis (SSc) is a rare connective-tissue disease of unknown origin affecting multiple organs. Characterized by autoimmunity, vessel inflammation, and organ fibrosis, SSc is classified by skin fibrosis extent into two patterns: limited cutaneous systemic sclerosis (lcSSc) and diffuse cutaneous systemic sclerosis (dcSSc). A significant complication of SSc is interstitial lung disease (ILD), which varies from slow to rapid progression [1–5]. Its clinical classification is based on the extent of skin fibrosis, which divides patients into two major patterns: limited cutaneous systemic sclerosis (lcSSc), which is characterised by skin fibrosis limited to the elbows and knees; and diffuse cutaneous systemic sclerosis, which involves proximal areas, the face, and the trunk in addition to distal areas [6, 7]. A main complication of SSc that contributes to morbidity is the appearance of interstitial lung disease (ILD) [8, 9]. The clinical course of SSc-associated interstitial lung disease (SSc-ILD) can range from a slowly progressing lung disease to a rapid progression [1]. The challenge, as with other ILDs [4], is identifying patients at high risk of progression and initiating early therapeutic intervention including immunosuppressive and/or antifibrotic therapy in order to limit disease extension and clinical flare up [2].

Biomarkers are crucial for quantifying ILD in SSc, providing insights into disease activity, severity, progression, and treatment response. They aid in early detection, risk stratification, distinguishing ILD subtypes, and guiding targeted treatment. Radiological ILD quantification on high-resolution CT (HRCT) is vital for monitoring disease progression, predicting outcomes, and identifying patients for early intervention [10]. However visual assessment of HRCT in ILD is prone to high inter-observer variability, poor reproducibility, and relative insensitivity to subtle disease progression over short follow-up periods. Machine learning models enhance HRCT assessments by accurately detecting and quantifying lung abnormalities, offering reproducible evaluations and reducing inter-observer variability. These models also provide objective treatment response measures, improving drug development and patient selection in clinical trials [11–20].

In this study, we investigate the automatic AI-based quantification of interstitial lung abnormalities from HRCT in SSc-ILD patients and their correlations with standard clinical markers like pulmonary function tests.

Methods

Patients cohort

We retrospectively analyzed 75 patients with SSc-ILD from the ILD clinic of University Hospital of Liège (CHU) seen between 9th of january 2007 to 30th of september 2022. Demographic data were collected (age, gender, BMI, tobacco status). Concerning systemic sclerosis classification, patients were classified according to the 2013 ACR/EULAR criteria for SSc [6] and the distinction of the cutaneous forms into limited and diffuse was made according to the classification of Leroy et al. [7]. Sine scleroderma are patients without cutaneous disease with other organ involvement. Concerning ILD classification, patients were classified as progressive pulmonary fibrosis if they met INBUILD criteria (PF-ILD) which was the definition used before 2022 [21]. Criteria for fibrotic progression of ILD were, on a follow-up period of 24 months before analysis:

- a relative decline in the forced vital capacity (FVC) of at least 10% of the predicted value;
- or a relative decline in the FVC of 5% to less than 10% of the predicted value and worsening of respiratory symptoms or an increased extent of fibrosis on high-resolution computed tomography (HRCT) of the chest;
- or worsening of respiratory symptoms and an increased extent of fibrosis on HRCT.

A total of 55 patients had longitudinal follow-up CT scans (between 2 and 4 scans), among which 23 were PF-ILD patients. The protocol was approved by ethics committee of CHU Liège, (Belgian number: B7072020000033) and all experiments were performed in accordance with relevant guidelines and regulations.

Pulmonary function tests

Lung function tests were performed in the routine respiratory laboratory at CHU Liège in accordance with the recommendations of the European Respiratory Society (ERS) [22]. Volumes are expressed in liter (L)(absolute value) and as percentage of predicted normal values. The Tiffeneau index or FEV1/FVC is expressed as percentage. The diffusion capacity of CO (DLCO) and carbon monoxide transfer coefficient (KCO or DLCO/VA) were measured by the single breath testing technique (Sensor Medics 2400 He / CO Analyzer System, Bilthoven, The Netherlands).

Statistical analysis

*P*arametric distribution of continuous variables were described using means and standard deviations (SD) and non-parametric distributions were described using median (interquartile range: IQR) expressed as number (% Yes). Spearman correlation coefficient (r) [23] was used for correlation between PFT and imaging parameters (strong correlation $r > 0.7$; moderate 0.3–0.7; low < 0.3). Paired T-test and Wilcoxon matched-pairs signed rank test for parametric and non-parametric variables respectively [24] were used for the longitudinal

analysis. The comparison between SSc-ILD and SSc-PFILD was analysed by unpaired T-test for FVC and DLCO and by Mann-Whitney test for TLV% and Severity score [25]. A p value less than 0.05 was accepted for statistical significance. Statistical analysis was performed using the TIBCO Statistica, v. 13.5.0, TIBCO Software Inc, Palo Alto, CA, USA and graphs using GraphPad Prism software version 9.0.0 for Windows, GraphPad Software, San Diego, California, USA software package.

Imaging parameters

All the CT images used in the study were acquired on one of the five multidetector CT scanners: Siemens Edge Plus (2), GE Revolution CT (1), and GE Brightspeed (2). Since CT images were collected retrospectively, no standardized scan protocol was available over the complete dataset. All scans were non-contrast High Resolution CT (slice thickness ≤ 1 mm) and acquired as per standard of care.

Icolung software

We employed the icolung software, which performs fully automatized segmentation of the lungs, lung lobes, and lung abnormalities (ground-glass opacity and consolidation) consecutively using deep learning models. These convolutional neural network models are based on the 2D and 3D U-net architectures described in [26, 27], and were trained, validated, and tested on clinical CT scans, along with voxel-level delineations of lung abnormalities, created by expert radiologists. Based on the models' predicted masks for lung abnormalities and lobes, the lung involvement in each lobe was computed as the ratio of abnormality volume vs. lobe volume, from which was derived a lobe-specific severity score (0–5). The five severity scores were then summed into a global severity score (0–25) for the patient's current CT exam. An example of the software report is depicted in Fig. 1. The software output consisted of Total Lung volume (TLV) (L), Lung abnormalities (combining consolidation and

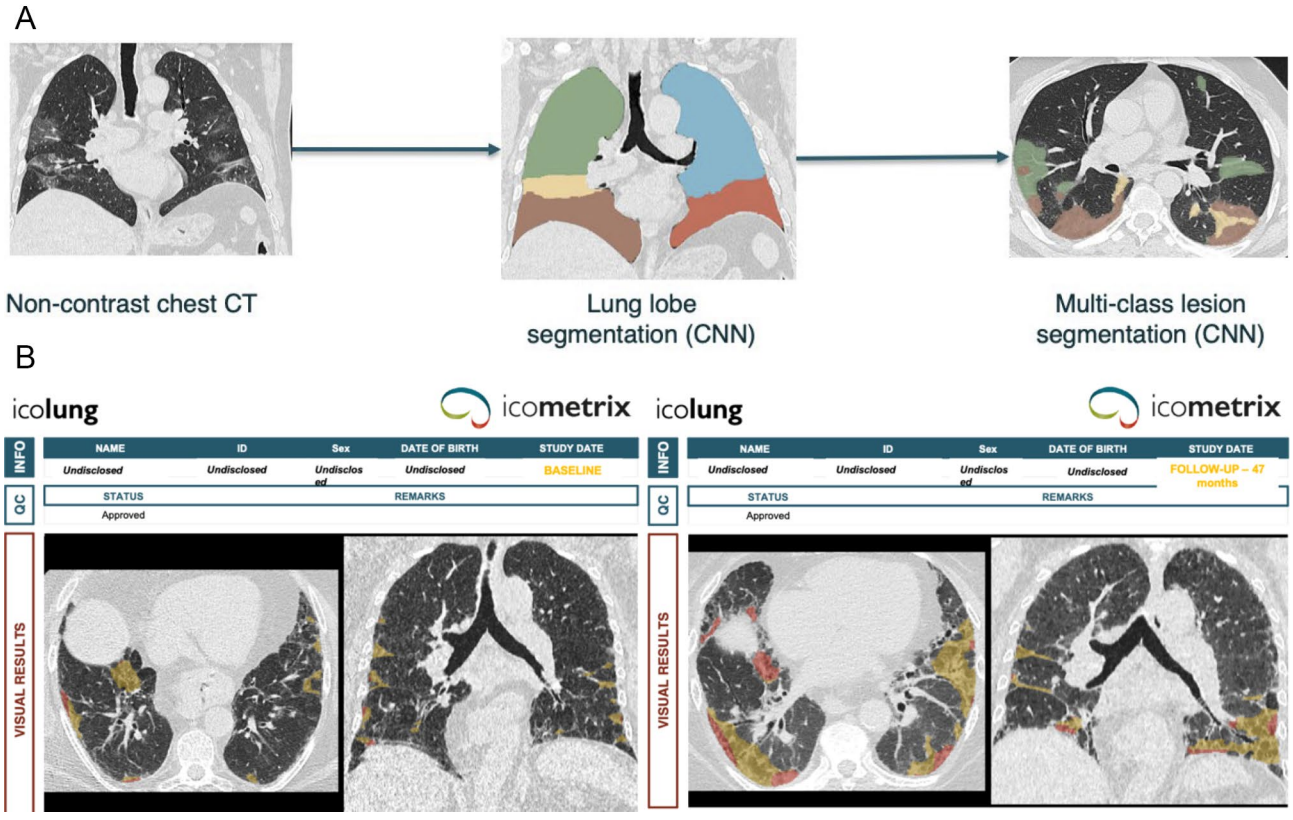

Fig. 1 **A**) Icolung software output combining the overall automatized lung segmentation (TLV quantification) and the association with lobar abnormalities. 3D analysis of parenchymal lung abnormalities: Coronal view illustrating automated lung segmentation and the visualization of abnormalities. The abnormalities are quantified using Icolung following lobe segmentation and represented with a conventional coronal view. The severity score is based on a five lung lobes scoring on a scale of 0 to 5, with 0 indicating no involvement (< 1%); 1, less than 5% involvement; 2, 5-25% involvement; 3, 26-49% involvement; 4, 50–75% involvement; and 5, more than 75% involvement. The total severity score is the sum of the individual lobar scores and range from 0 (no involvement) to 25 (maximum involvement). (**B**) Screenshots of the Icolung analysis report from baseline (left) and follow up scan (right) of SSc female patient, SCL-70 + treated with MMF exhibiting a PPF phenotype. FVC and DLCO (in % predicted) were 103% and 60% at baseline versus 60% and 28% at follow-up respectively. The 3D segmentation masks of the abnormalities are visualized in 2D axial and coronal views (red = consolidation, yellow = ground glass opacities)

ground-glass opacities)(% of TLV), Consolidation (% of TLV), Ground-Glass Opacities (% TLV) and severity score per patient.

Results

The baseline clinical, functional and imaging parameters of the patients are reported in Table 1. P values are reported for statistically significant differences between the SSc-ILD and SSc-PFILD groups.

The correlation between the lesion percentage out of the total lung volume (Lesion %) and the results of the pulmonary function tests (FVC and DLCO) is reported in Fig. 2. Both lung FVC and DLCO had a significant correlation with the lesion extent percentage extracted from the image analysis (r=-0.50 and r=-0.46 respectively). The complete correlation analysis is reported in Table S1.

The comparison between SSc-ILD and SSc-PFILD patients is reported in Fig. 3. Statistically significant differences were found between the two groups in terms of FVC (Fig. 3A), TLV% (Fig. 3B) and Severity score (Fig. 3D). Differences in DLCO values were not statistically significant (Fig. 3C).

Patients with SSc-PFILD displayed a higher extent of lesions out of the Total Lung Volume (% TLV): 3.93 (0.36–8.12) versus 0.59 (0.09–3.53)($p<0.05$) and a higher Severity score: 4 (1–6) versus 1 (0–4) than those of the SSc-ILD group ($p<0.05$). Pulmonary functional tests showed a marked decrease in FVC: 77 ± 20% pred. for

Table 1 Patients' clinical, functional characteristics and imaging-based quantifications

Demography	ALL	SSc-ILD	SSc-PFILD	*P* value
	N = 75	*N* = 45	*N* = 30	
Age, years	55 (47–69)	58 (44–70)	53(47–65)	0.9147
Gender (M/F)	25/50 (33%)	11/34 (24%)	14/16 (52%)	0.0789
BMI, Kg/m^2	25.1 ± 4.2	24.0 ± 5.1	25.0 ± 6.5	0.4804
Smokers NS/FS/CS (%)	51%/28%/22%	49%/28%/23%	54%/27%/19%	0.8629
Limited SSc/dcSSc/sine scleroderma (N)	56/12/7	36/2/7	20/10/0***	**0.0009**
Positive Anti-scl-70	10 (14%)	6(13%)	4 (14%)	> 0.9999
Pulmonary function test				
FEV-1 (L)	2.29 ± 0.72	2.3 ± 0.69	2.27 ± 0.77	0.837
FEV-1 (% pred.)	83 ± 19	86 ± 18	77 ± 19	0.035
FVC (L)	2.83 ± 0.92	2.86 ± 0.87	2.79 ± 1.02	0.767
FVC (% pred.)	83 ± 20	87 ± 19	77 ± 20*	**0.023**
FEV1/FVC (Tiffeneau index)(%)	81 ± 7	82 ± 7	82 ± 7	0.529
MEF25-75 (L/s)	2.45 ± 0.94	2.45 ± 0.94	2.46 ± 0.95	0.770
MEF25-75 (%)	83 ± 27	86 ± 29	79 ± 24	0.343
TLC (L)	4.53 ± 1.28	4.64 ± 1.26	4.37 ± 1.32	0.342
TLC (% pred.)	81 ± 18	86 ± 19	73 ± 16**	**0.002**
RV (L)	1.74 ± 0.72	1.74 ± 0.74	1.72 ± 0.72	0.798
RV (% pred.)	88 ± 34	92 ± 37	82 ± 30	0.103
FRC (L)	2.94 ± 0.97	2.97 ± 1.02	2.89 ± 0.93	0.597
FRC (% pred.)	98 ± 29	102 ± 32	92 ± 24	0.133
DLCO (mmol.min^{-1}.Kpa^{-1})	4.62 ± 1.83	4.63 ± 1.84	4.6 ± 1.84	0.836
DLCO (% pred.)	54 ± 18	56 ± 19	52 ± 17	0.553
KCO (mmol.min^{-1}.Kpa^{-1}.L^{-1})	1.14 ± 0.29	1.13 ± 0.31	1.16 ± 0.26	0.354
KCO (% pred.)	76 (68–86)	76 (65–83)	77 (69–86)	0.213
sGaw (L.sec^{-1}.kPa^{-1}.L^{-1})	1.23 ± 0.67	1.14 ± 0.6	1.37 ± 0.74	0.107
sGaw (% pred.)	86 ± 45	74 ± 35	103 ± 52*	**0.046**
CT Scan analysis				
ILA out of lung volume (TLV in ml)	4028 (3327–5108)	4043 (3286–5004)	4024 (3330–5171)	0.952
TLV (%)	1.35 (0.1–5.89)	0.59 (0.09–3.53)	3.93 (0.36–8.12)*	**0.035**
Consolidation (%)	0.12 (0.01–0.87)	0.05 (0-0.28)	0.46 (0.03–1.59)*	**0.023**
Ground glass opacities (%)	1.06 (0.09–4.23)	0.5 (0.07–2.95)	2.97 (0.32–4.87)	0.092
Global severity score	2 (0–6)	1 (0–4)	4 (1–6)*	**0.017**

Data are expressed as mean ± SD and median (IQR) for parametric and non-parametric variables respectively. SSc-PFILD: SSc patients with PPF, NS/FS/CS: Non-smokers/Former Smokers/Current smokers, lcSSc: limited cutaneous systemic sclerosis, dcSSc: diffuse cutaneous systemic sclerosis, ILA: Interstitial lung abnormalities, FEV1: Forced expired volume in one second, FVC: Forced vital capacity, MEF20-75: Maximal expiratory flow, TLC: Total Lung Capacity, RV: Residual volume, FRC: Functional residual capacity, DLCO: Diffusing lung capacity for CO, KCO: Carbon monoxide transfer coefficient, sGaw: Specific airways conductance, TLV: Total lung volume

Chest CT lesions quantifications were performed with ICOLUNG software

Valid N for TLC; RV; FRC; DLCO; KCO; sGaw (L.sec^{-1}.kPa^{-1}.L^{-1}); sGaw(% pred.) were respectively 68-67-63-71-62-34-20

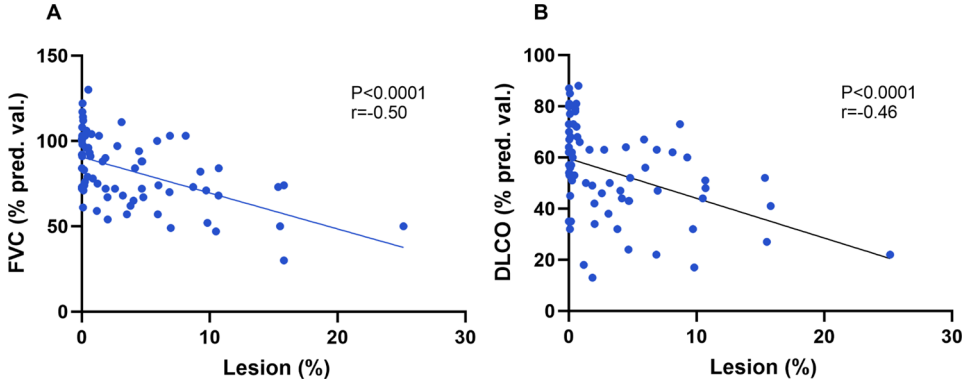

Fig. 2 Correlation between IA quantification of lesions and functional parameters. Correlation between percentage of lesions quantified out of the TLV from the AI algorithm with FVC (**A**) and DLCO (**B**)

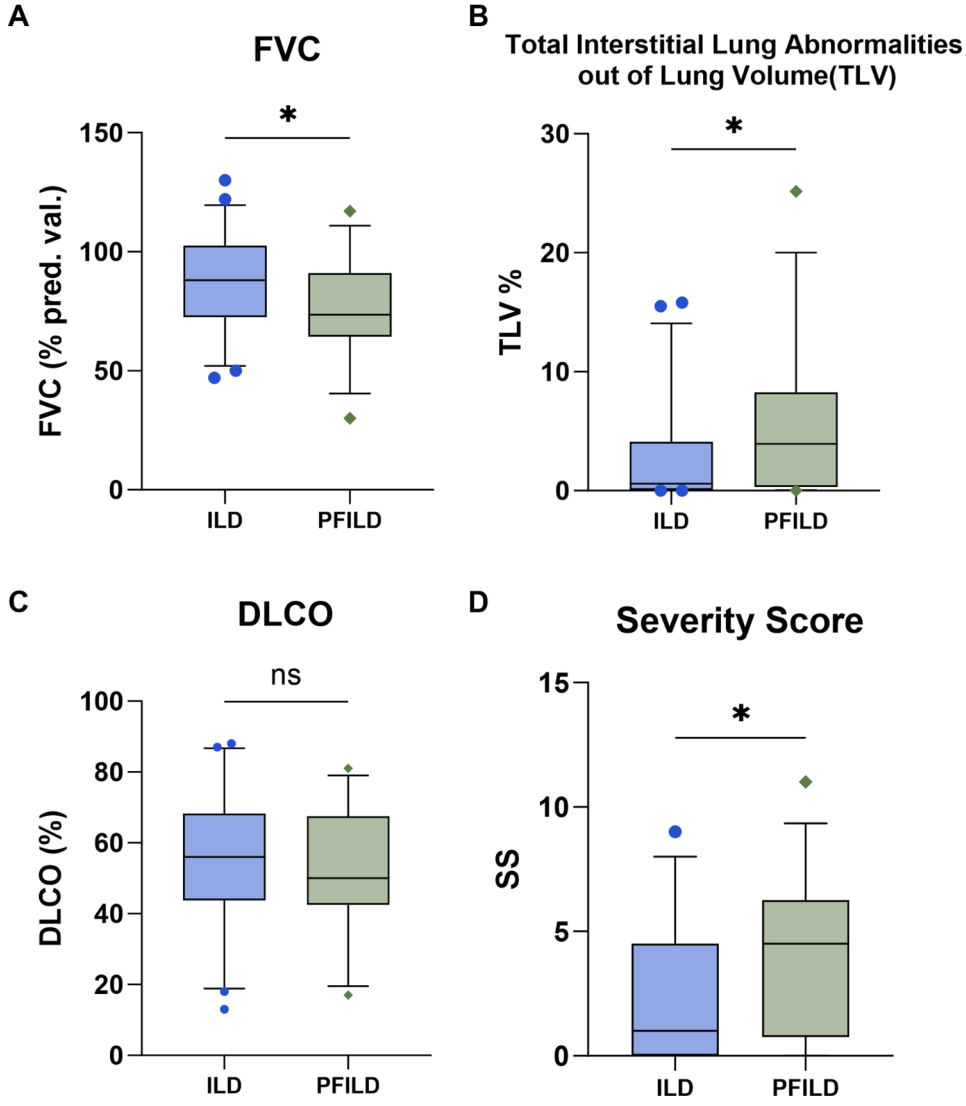

Fig. 3 Comparison between functional and imaging biomarkers in SSc-ILD and SSc-PFILD. Difference in FVC (**A**), TLV% (**B**), DLCO (**C**) and Severity score (**D**) for patients with SSc-ILD (blue bar) and SSc-PFILD (green bar). Data was analyzed by unpaired T test for FVC and DLCO and by Mann Whitney test for TLV and Severity score. *p value < 0.05

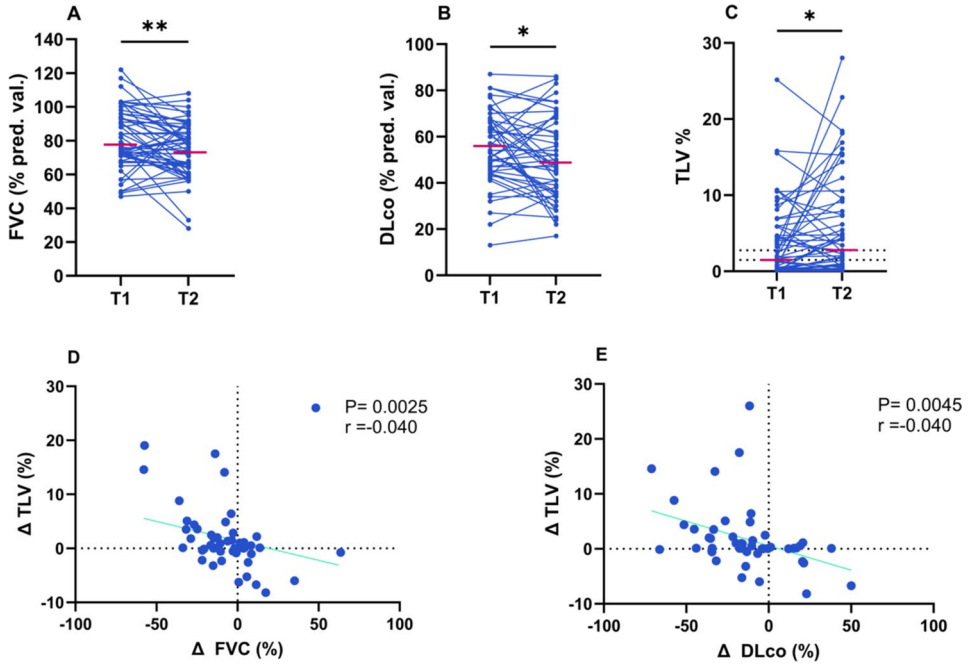

Fig. 4 ILD quantification compared to PFT modifications over time. **A.B.C.** Variation over time of FVC (**A**), DLCO (**B**) and TLV % (**C**). Data was analyzed by the paired T test for FVC and DLCO and by the Wilcoxon matched-pairs signed rank test for TLV %. T1 and T2 represent the two different timepoints for CT-scan analysis *P value < 0.05 ;**P value < 0.01. **D.E.** Correlation between the variation over the time of FVC (**D**) and DLCO ($n = 48$)(**E**) correlated with ILD progression over time out of the total lung volume (TLV %)

SSc-PFILD in comparison to the other group (FVC: 87 ± 19% pred.)($p < 0.05$). The complete results of the comparison tests are reported in Table S1 for the imaging parameters and PFTs.

A subsequent analysis was performed on 55 patients with longitudinal data (32 SSc-ILD and 23 SSc-PFILD), considering T1 as the scan at diagnosis and T2 as follow-up scan. Figure 4 reports the variation over time of FVC (Fig. 4A), DLCO (Fig. 4B) and TLV% (Fig. 4C). The variation over T1 and T2 of TLV% showed moderate correlation with both the variation of FVC (r= -0.40, $p < 0.01$) and DLCO ($n = 48$)(r= -0.40, $p < 0.01$) in Fig. 4D and E, respectively. The mean follow-up was 3.9 years (1.8–6.7) ($p = 0.45$). The complete correlation analysis is reported in Table S1.

Discussion

Quantification of interstitial lung disease on CT scans is still challenging for clinicians. Qualitative and semi-quantitative visual assessments of disease extent in ILDs have been adopted, the latter striving for quantification and standardization of the evaluation of disease extent in comparison to the former. However, both approaches suffer from moderate to high inter-reader variability (kappa value ranging from 0.28 to 0.85) [28], necessitate description of the location of the abnormalities allowing a basic quantification of ILD severity [29–31].

The differentiation of the abnormalities and the grading of each abnormal area still remains a challenge. Several different abnormalities can be present in ILD patients and even the most common, namely ground glass opacities (GGO), consolidation, reticulation and honeycombing, are difficult to differentiate and correctly attribute [32]. Moreover, these qualitative and semi-quantitative approaches are time consuming, dependent on radiological expertise and prone to manual errors. In the present manuscript, we describe the application of an automated, reproducible, and accurate quantification tool that can help radiologists and clinicians overcome these limitations, allowing a fully quantitative approach.

Novel solutions to unburden clinical staff, to help in the diagnosis process and evaluation of changes over time represent an urgent clinical need. In the last years, several additional deep learning (DL) methods have been put out for the purpose of identifying and quantifying lung abnormalities [33, 34], which can be then used to ILD lesions [35, 36], highlighting the potential benefits of this approach in the management of patients with restrictive lung diseases. Furthermore, several studies have reported correlations between this automatic AI-based quantification of lung abnormalities and PFT parameters used in standard of care clinical practice for diagnosis and follow up. Si-Moahmed et al. [37] used a commercially available software tool to measure the lung CT volume and correlate this with FVC and total lung capacity (TLC). Sue

et al. [38] explored the correlation between abnormalities pattern volume and vasculature volume with PFT parameters in a cohort of idiopathic pulmonary fibrosis (IPF) patients. In the specific scenario of SSc-related ILDs, Karadag et al. [39] investigated automatic extraction of textural lung features and their relationship to pulmonary function tests and visual fibrosis scores (VFS), finding moderate to strong correlations, and a notable distinction between PF and non-PF patients.

Our novel approach investigates the temporal progression of both progressive and non-progressive SSc-ILD patients, which is, to our knowledge, the first study to do so. It also clearly establishes a correlation between automatic volumetric quantification of abnormalities and PFTs, enabling the characterization and distinction of both groups of patients. The ability to follow this change over time is of the utmost importance for therapy planning and follow-up, and it might promote the development of innovative imaging-based endpoints in clinical trials when evaluating effectiveness of antifibrotic medications [40, 41]. Adding automatized HRCT quantification tools in patients follow-up is of major interest as a clinical decision support companion aiming to reliably help clinicians in patients management.

The present approach combining AI-based image analysis and AI, tackles three of the key challenges in the management of ILD patients: early diagnosis, accurate prognostication from baseline scans and therapy response monitoring over time [42]. The automatic quantification of lung abnormalities could in turn streamline and simplify current classification criteria for ILDs, distinguishing between limited and extensive disease in a quantitative, robust and reproducible way, for example with an improved Goh algorithm for optimal prognosis of SSc-ILD patients [43, 44]. Moreover, the correlations between both PFTs and imaging parameters in the cohort of progressive versus non progressive patients, may pave the road for the future development of an integrated and automated image analysis tool able to predict patients with higher risk of developing PPF [45, 46]. This will improve patients' management and result in better quality of life, when therapies can be delivered faster and more efficiently in a context of personalized medicine.

The current study has some limitations. The data are monocentric and retrospectively collected, so there is no homogenous image acquisition protocol nor scan acquisition timeline. Moreover, we also included patients with limited lung involvement (< 10%) in the cohort. While this represents better the reality of clinical practice, the lack of homogeneous imaging parameters and comparable scan acquisition times might have reduced the performance and affect especially the longitudinal analysis and the overall correlation PFTs. We also used the PFILD definition as the patients were clinically classified before the publication of the guidelines. Nevertheless, the case review confirmed that all patients were also presenting the new PPF criteria. A prospective trial is envisioned in the future to provide more homogeneous data collecting and potentially extent longitudinal analysis to more than one follow-up scan. In addition, the current version of the software identifies and quantifies only ground glass opacities and consolidation. However, some reports in literature indicate variables correlations between other abnormal patterns and PFTs results, for example reticulation which seems to be correlated with DLCO (r = -0.581) [47, 48]. Taking into account other abnormalities patterns in future analysis might refine even more the diagnostic and prognostic approach based on automatic AI quantification from chest CT scans.

Conclusion

Quantitative metrics obtained from AI-driven analysis of chest CT images in SSc-ILD has shown promising results in the correlations with PFTs, supporting quantifiable and reproducible disease evaluation. This approach holds the potential to improve the management of SSc-ILD patients. However, prior to its integration into routine clinical practice, it is necessary to perform comprehensive clinical multicentric studies to validate the model outcomes and their correlation with standard of care PFTs. Along with this effort, we need to elucidate its ability to accurately predict patient outcomes, especially regarding the insurgence of progressive pulmonary fibrosis. The possibility of predicting PPF from baseline scans as well as response to therapy is an urgent clinical unmet need in the field of SSc-ILD.

Abbreviations

CT	Computed tomography
CNN	Convolutional Neural Network
DLCO	Diffusing lung capacity for CO
FEV-1	Forced expired volume in one second
FRC	Functional residual capacity
FVC	Forced vital capacity
GGO	Ground glass opacities
ILA	Interstitial lung abnormalities
ILD	interstitial lung disease
IPF	Idiopathic pulmonary fibrosis
IQR	interquartile range
KCO	Carbon monoxide transfer coefficient
lcSSc	limited cutaneous systemic sclerosis
dcSSc	Diffuse cutaneous systemic sclerosis
MEF20-75	Maximal expiratory flow
PFT	Pulmonary function test
PPF	Progressive pulmonary fibrosis
RV	Residual volume
SD	Standard deviations
sGaw	Specific airways conductance
SSc	Systemic sclerosis
TLC	Total Lung Capacity
TLV	Total lung volume
VFS	Visual fibrosis scores

Supplementary Information

The online version contains supplementary material available at https://doi.org/10.1186/s12931-025-03117-9.

Supplementary Material 1

Acknowledgements
We thank Dr Marie ERNST from the biostatistical department for her help in statistical analysis and review.

Author contributions
JG and RL conceived the study. MH, JG and SVE analyzed the results. MH performed statistical analysis. JG, FG, BA, A-NF and CR conducted the experiments and acquired the data. BE acquired the funding. DS and SVE provided the icolung software. JG, BE, A-NF, SVE, GY, SW, VC and VS wrote the manuscript. KA, LC, JGS, HS, JS, IT, VC and ST reviewed and validated the manuscript.

Funding
This work was supported by the European Respiratory Society – Clinical Research Collaboration program through the *PROFILE.net* project and by a FIRS grant (University Hospital of Liège).

Data availability
No datasets were generated or analysed during the current study.

Declarations

Ethics approval and consent to participate
The study was approved by the University Hospital of Liege Institutional Review Board (7072020000033). Consent to participate was waived considering the retrospective nature of the study.

Consent for publication
Not applicable.

Clinical trial number
Not applicable.

Competing interests
D.S. is an employee and shareholder of icometrix. S.VE is an employee of icometrix.

Author details
[1]Department of Respiratory Medicine, University Hospital of Liège, Liège, Belgium
[2]Department of Rheumatology, University Hospital of Liège, Liège, Belgium
[3]icometrix, Leuven, Belgium
[4]Laboratory of Cellular and Molecular Pneumonology, School of Medicine, University of Crete, Heraklion, Crete, Greece
[5]Department of Respiratory Medicine, Maastricht University Medical Centre, Maastricht, the Netherlands
[6]Department of Rheumatology and Immunology, Department of Pulmonary Medicine, Inselspital, Bern University Hospital, University of Bern, Bern, Switzerland
[7]Department for BioMedical Research (DBMR), Lung Precision Medicine (LPM), University of Bern, Bern, Switzerland
[8]Department of Pneumology, ZNA Middelheim, Antwerpen, Belgium
[9]Mainz Center for Pulmonary Medicine, Department of Pneumology, Department of Pulmonary, ZfT, Mainz University Medical Center and Department of Pulmonary, Critical Care and Sleep Medicine, Marienhaus Clinic Mainz, Mainz, Germany
[10]Department of Pneumology, Hospital Clínic-Universitat de Barcelona, Barcelona, Spain
[11]Department of Pulmonary Medicine, SOTIRIA Chest Diseases Hospital of Athens, Athens, Greece
[12]Bioengineering Department and Imperial-X, Imperial College London, London, UK
[13]National Heart and Lung Institute, Imperial College London, London, UK
[14]National Reference Centre for Rare Pulmonary Diseases, Louis Pradel Hospital, member of ERN-LUNG, Hospices Civils de Lyon, UMR 754, INRAE, Claude Bernard University Lyon 1, Lyon, France
[15]Unit of Interventional Pulmonology, Department of Experimental and Clinical Medicine, Careggi University Hospital, Florence, Italy
[16]Department of Rheumatology, Ghent University Hospital, Ghent, Belgium
[17]Department of Internal Medicine, Ghent University, Ghent, Belgium
[18]Unit for Molecular Immunology and Inflammation, VIB Inflammation Research Centre (IRC), Ghent, Belgium

Received: 18 July 2024 / Accepted: 13 January 2025
Published online: 24 January 2025

References

1. Cottin V, Brown KK. Interstitial lung disease associated with systemic sclerosis (SSc-ILD). Respir Res Engl. 2019;20:13.
2. Vonk MC, Smith V, Sfikakis PP, Cutolo M, Del Galdo F, Seibold JR. Pharmacological treatments for SSc-ILD: systematic review and critical appraisal of the evidence. Autoimmun Rev Neth. 2021;20:102978.
3. Levin D, Osman MS, Durand C, Kim H, Hemmati I, Jamani K, et al. Hematopoietic cell transplantation for systemic Sclerosis-A review. Switzerland: Cells; 2022. p. 11.
4. Fischer A, du Bois R. Interstitial lung disease in connective tissue disorders. Lancet (London, England). Engl; 2012;380:689–98.
5. O'Reilly S. Metabolic perturbations in systemic sclerosis. Curr Opin Rheumatol United States. 2022;34:91–4.
6. van den Hoogen F, Khanna D, Fransen J, Johnson SR, Baron M, Tyndall A, et al. 2013 classification criteria for systemic sclerosis: an American college of rheumatology/European league against rheumatism collaborative initiative. Ann Rheum Dis Engl. 2013;72:1747–55.
7. LeRoy EC, Black C, Fleischmajer R, Jablonska S, Krieg T, Medsger TAJ, et al. Scleroderma (systemic sclerosis): classification, subsets and pathogenesis. J Rheumatol Can. 1988;15:202–5.
8. Khanna D, Tashkin DP, Denton CP, Renzoni EA, Desai SR, Varga J, Etiology. Risk factors, and biomarkers in systemic sclerosis with interstitial lung disease. Am J Respir Crit Care Med United States. 2020;201:650–60.
9. Moinzadeh P, Bonella F, Oberste M, Weliwitage J, Blank N, Riemekasten G, et al. Impact of systemic sclerosis-Associated interstitial lung Disease With and without Pulmonary Hypertension on Survival: a large cohort study of the German Network for systemic sclerosis. Chest. 2024;165(1):132–45.
10. Distler O, Assassi S, Cottin V, Cutolo M, Danoff SK, Denton CP et al. Predictors of progression in systemic sclerosis patients with interstitial lung disease. Eur Respir J Engl; 2020;55.
11. Dack E, Christe A, Fontanellaz M, Brigato L, Heverhagen JT, Peters AA, et al. Artificial Intelligence and interstitial lung disease: diagnosis and prognosis. Invest Radiol United States. 2023;58:602–9.
12. Soffer S, Morgenthau AS, Shimon O, Barash Y, Konen E, Glicksberg BS, et al. Artificial Intelligence for Interstitial Lung Disease Analysis on chest computed tomography: a systematic review. Acad Radiol Elsevier. 2022;29:S226–35.
13. Handa T, Tanizawa K, Oguma T, Uozumi R, Watanabe K, Tanabe N, et al. Novel Artificial Intelligence-based technology for chest computed Tomography Analysis of Idiopathic Pulmonary Fibrosis. Ann Am Thorac Soc United States. 2022;19:399–406.
14. Frix A-N, Cousin F, Refaee T, Bottari F, Vaidyanathan A, Desir C et al. Radiomics in Lung diseases Imaging: state-of-the-art for clinicians. J Pers Med. 2021.
15. Schniering J, Maciukiewicz M, Gabrys HS, Brunner M, Blüthgen C, Meier C et al. Computed tomography-based radiomics decodes prognostic and molecular differences in interstitial lung disease related to systemic sclerosis. Eur Respir J Engl; 2022;59.
16. Martini K, Baessler B, Bogowicz M, Blüthgen C, Mannil M, Tanadini-Lang S, et al. Applicability of radiomics in interstitial lung disease associated with systemic sclerosis: proof of concept. Eur Radiol Ger. 2021;31:1987–98.
17. Walsh SLF, Calandriello L, Silva M, Sverzellati N. Deep learning for classifying fibrotic lung disease on high-resolution computed tomography: a case-cohort study. Lancet Respir Med. Else; 2018;6:837–45.
18. Bonhomme O, André B, Gester F, de Seny D, Moermans C, Struman I, et al. Biomarkers in systemic sclerosis-associated interstitial lung disease: review of the literature. Rheumatol (Oxford) Engl. 2019;58:1534–46.

19. Makol A, Nagaraja V, Amadi C, Pugashetti JV, Caoili E, Khanna D. Recent innovations in the screening and diagnosis of systemic sclerosis-associated interstitial lung disease. Expert Rev Clin Immunol Engl. 2023;19:613–26.
20. Hoffmann-Vold A-M, Maher TM, Philpot EE, Ashrafzadeh A, Distler O. Assessment of recent evidence for the management of patients with systemic sclerosis-associated interstitial lung disease: a systematic review. ERJ open Res Engl. 2021;7.
21. Flaherty KR, Wells AU, Cottin V, Devaraj A, Walsh SLF, Inoue Y, et al. Nintedanib in progressive fibrosing interstitial lung diseases. N Engl J Med. 2019;381:1718–27.
22. Stanojevic S, Kaminsky DA, Miller M, Thompson B, Aliverti A, Barjaktarevic I et al. ERS/ATS technical standard on interpretive strategies for routine lung function tests. Eur Respir J. 2021;2101499.
23. Schober P, Boer C, Schwarte LA. Correlation coefficients: appropriate use and interpretation. Anesth Analg. 2018;126.
24. MacFarland TW, Yates JM. In: MacFarland TW, Yates JM, editors. Wilcoxon matched-pairs signed-ranks test BT - introduction to nonparametric statistics for the Biological sciences using R. Cham: Springer International Publishing; 2016. pp. 133–75.
25. Fay MP, Proschan MA. Wilcoxon-Mann-Whitney or t-test? On assumptions for hypothesis tests and multiple interpretations of decision rules. Stat Surv. 2010;4:1–39.
26. Çiçek Ö, Abdulkadir A, Lienkamp SS, Brox T, Ronneberger O. 3D U-net: learning dense volumetric segmentation from sparse annotation. Lect Notes Comput Sci (including Subser Lect Notes Artif Intell Lect Notes Bioinformatics). 2016.
27. Ronneberger O, Fischer P, Brox T. In: Navab N, Hornegger J, Wells WM, Frangi AF, editors. U-Net: Convolutional Networks for Biomedical Image Segmentation BT - Medical Image Computing and Computer-assisted intervention – MICCAI 2015. Cham: Springer International Publishing; 2015. pp. 234–41.
28. Widell J, Lidén M. Interobserver variability in high-resolution CT of the lungs. Eur J Radiol Open. 2020;7:100228.
29. Watadani T, Sakai F, Johkoh T, Noma S, Akira M, Fujimoto K, et al. Interobserver Variability in the CT Assessment of Honeycombing in the lungs. Radiol Radiological Soc North Am. 2013;266:936–44.
30. Aziz ZA, Wells AU, Hansell DM, Bain GA, Copley SJ, Desai SR, et al. HRCT diagnosis of diffuse parenchymal lung disease: inter-observer variation. Thorax. 2004;59:506–11.
31. Occhipinti M, Bosello S, Sisti LG, Cicchetti G, de Waure C, Pirronti T, et al. Quantitative and semi-quantitative computed tomography analysis of interstitial lung disease associated with systemic sclerosis: a longitudinal evaluation of pulmonary parenchyma and vessels. PLoS ONE. 2019;14:1–18.
32. Axelsson GT, Gudmundsson G. Interstitial lung abnormalities - current knowledge and future directions. Eur Clin Respir J. 2021;8:1994178.
33. Agarwala S, Kale M, Kumar D, Swaroop R, Kumar A, Kumar Dhara A et al. Deep learning for screening of interstitial lung disease patterns in high-resolution CT images. Clin Radiol. The Royal College of Radiol; 2020;75:481.e1-481.e8.
34. Mergen V, Kobe A, Blüthgen C, Euler A, Flohr T, Frauenfelder T et al. Deep learning for automatic quantification of lung abnormalities in COVID-19 patients: first experience and correlation with clinical parameters. Eur J Radiol Open. 2020;7.
35. Walsh SLF, Calandriello L, Silva M, Sverzellati N. Deep learning for classifying fibrotic lung disease on high-resolution computed tomography: a case-cohort study. Lancet Respir Med. Else; 2018;6:837–45.
36. Ho TT, Kim T, Kim WJ, Lee CH, Chae KJ, Bak SH, et al. A 3D-CNN model with CT-based Parametric response mapping for classifying COPD subjects. Sci Rep Nat Publishing Group UK. 2021;11:1–12.
37. Si-Mohamed SA, Nasser M, Colevray M, Nempont O, Lartaud P-J, Vlachomitrou A, et al. Automatic quantitative computed tomography measurement of longitudinal lung volume loss in interstitial lung diseases. Eur Radiol. 2022;32:4292–303.
38. Sun H, Liu M, Kang H, Yang X, Zhang P, Zhang R, et al. Quantitative analysis of high-resolution computed tomography features of idiopathic pulmonary fibrosis: a structure-function correlation study. Quant Imaging Med Surg China. 2022;12:3655–65.
39. Temiz Karadag D, Cakir O, San S, Yazici A, Ciftci E, Cefle A. Association of quantitative computed tomography ındices with lung function and extent of pulmonary fibrosis in patients with systemic sclerosis. Clin Rheumatol. 2022;41:513–21.
40. Barnes H, Humphries SM, George PM, Assayag D, Glaspole I, Mackintosh JA, et al. Machine learning in radiology: the new frontier in interstitial lung diseases. Lancet Digit Heal Engl. 2023;5:e41–50.
41. Nathan SD, Meyer KC. IPF clinical trial design and endpoints. Curr Opin Pulm Med United States. 2014;20:463–71.
42. Cottin V. Interstitial lung disease: new challenges and evolving phenotypes. Eur Respir Rev. 2010;19:91 LP – 93.
43. Goh NSL, Desai SR, Veeraraghavan S, Hansell DM, Copley SJ, Maher TM, et al. Interstitial lung disease in systemic sclerosis: a simple staging system. Am J Respir Crit Care Med United States. 2008;177:1248–54.
44. Jeny F, Brillet P-Y, Kim Y-W, Freynet O, Nunes H, Valeyre D. The place of high-resolution computed tomography imaging in the investigation of interstitial lung disease. Expert Rev Respir Med. Taylor & Francis; 2019;13:79–94.
45. Nagy T, Toth NM, Palmer E, Polivka L, Csoma B, Nagy A, et al. Clinical predictors of lung-function decline in systemic-sclerosis-Associated interstitial lung disease patients with normal spirometry. Biomedicines. Switzerland; 2022. p. 10.
46. Li L, Gao S, Fu Q, Liu R, Zhang Y, Dong X, et al. A preliminary study of lung abnormalities on HRCT in patients of rheumatoid arthritis–associated interstitial lung disease with progressive fibrosis. Clin Rheumatol. 2019;38:3169–78.
47. Kazantzi A, Costaridou L, Skiadopoulos S, Korfiatis P, Karahaliou A, Daoussis D, et al. Automated 3D Interstitial Lung Disease Extent quantification: performance evaluation and correlation to PFTs. J Digit Imaging. 2014;27:380–91.
48. Occhipinti M, Bruni C, Camiciottoli G, Bartolucci M, Bellando-Randone S, Bassetto A et al. Quantitative analysis of pulmonary vasculature in systemic sclerosis at spirometry-gated chest CT. Ann Rheum Dis. 2020;79:1210–17.

Publisher's note